Cardiovascular Research
doi:10.1093/cvr/cvt341

Fatty acid nitroalkenes ameliorate glucose intolerance and pulmonary hypertension in high-fat diet-induced obesity

Eric E. Kelley[1,2], Jeff Baust[2], Gustavo Bonacci[3], Franca Golin-Bisello[3], Jason E. Devlin[4], Claudette M. St. Croix[4], Simon C. Watkins[4], Sonia Gor[3], Nadiezhda Cantu-Medellin[2], Eric R. Weidert[1], Jefferson C. Frisbee[5], Mark T. Gladwin[2,6], Hunter C. Champion[2,6], Bruce A. Freeman[2,3]*, and Nicholas K.H. Khoo[3]*

[1]Department of Anesthesiology, University of Pittsburgh, Pittsburgh, PA, USA; [2]Vascular Medicine Institute, University of Pittsburgh, Pittsburgh, PA, USA; [3]Department of Pharmacology and Chemical Biology, University of Pittsburgh, Thomas E. Starzl Biomedical Science Tower-E1340, 200 Lothrop St, Pittsburgh, PA 15213, USA; [4]Center for Biological Imaging, University of Pittsburgh, Pittsburgh, PA, USA; [5]Department of Physiology and Pharmacology, West Virginia University Health Sciences Center, Morgantown, WV, USA; and [6]Department of Medicine, University of Pittsburgh, Pittsburgh, PA, USA

Received 4 August 2013; revised 10 December 2013; accepted 19 December 2013

Time for primary review: 19 days

Aims Obesity is a risk factor for diabetes and cardiovascular diseases, with the incidence of these disorders becoming epidemic. Pathogenic responses to obesity have been ascribed to adipose tissue (AT) dysfunction that promotes bioactive mediator secretion from visceral AT and the initiation of pro-inflammatory events that induce oxidative stress and tissue dysfunction. Current understanding supports that suppressing pro-inflammatory and oxidative events promotes improved metabolic and cardiovascular function. In this regard, electrophilic nitro-fatty acids display pleiotropic anti-inflammatory signalling actions.

Methods and results It was hypothesized that high-fat diet (HFD)-induced inflammatory and metabolic responses, manifested by loss of glucose tolerance and vascular dysfunction, would be attenuated by systemic administration of nitrooctadecenoic acid ($OA\text{-}NO_2$). Male C57BL/6j mice subjected to a HFD for 20 weeks displayed increased adiposity, fasting glucose, and insulin levels, which led to glucose intolerance and pulmonary hypertension, characterized by increased right ventricular (RV) end-systolic pressure (RVESP) and pulmonary vascular resistance (PVR). This was associated with increased lung xanthine oxidoreductase (XO) activity, macrophage infiltration, and enhanced expression of pro-inflammatory cytokines. Left ventricular (LV) end-diastolic pressure remained unaltered, indicating that the HFD produces pulmonary vascular remodelling, rather than LV dysfunction and pulmonary venous hypertension. Administration of $OA\text{-}NO_2$ for the final 6.5 weeks of HFD improved glucose tolerance and significantly attenuated HFD-induced RVESP, PVR, RV hypertrophy, lung XO activity, oxidative stress, and pro-inflammatory pulmonary cytokine levels.

Conclusions These observations support that the pleiotropic signalling actions of electrophilic fatty acids represent a therapeutic strategy for limiting the complex pathogenic responses instigated by obesity.

Keywords Obesity • Pulmonary hypertension • Nitro-fatty acid signalling • Inflammation • Xanthine Oxidase

1. Introduction

Obesity affects >1.5 billion people worldwide and is a risk factor for insulin resistance, Type 2 diabetes mellitus (T2DM), and cardiovascular diseases (CVDs). Obesity, defined by excess adipose tissue (AT) mass with accumulation of fat into peripheral organs, is now recognized as a chronic, low-grade inflammatory disease. Obesity-induced pro-inflammatory signalling cascades promote AT dysfunction and adipokine dysregulation which, in turn, lends resistance to salutary signalling molecules, such as insulin and leptin. Therefore, weight loss would be predicted to have beneficial effects on insulin resistance and complications associated T2DM, such as CVDs.

* Corresponding author. Tel: +1 412 648 9319; fax: +1 412 648 2229, Email: freerad@pitt.edu (B.A.F.), nkhoo@pitt.edu (N.K.H.K.)

Obesity-induced adipokine dysfunction promotes systemic vasculopathies including atherosclerosis and hypertension, as well as pulmonary diseases including asthma, chronic obstructive pulmonary disease, and pulmonary hypertension (PH).[1–3] Notably, PH affects both the systemic and pulmonary vasculature and is characterized by vasoconstriction, vascular proliferation, and remodelling of small pulmonary arteries. This increases pulmonary vascular resistance (PVR), pulmonary arterial pressure (PAP), and right ventricular (RV) end-systolic pressure (RVESP), causing pulmonary arterial obstruction.[4] The right ventricle compensates to preserve cardiac output (CO) by undergoing hypertrophy and eventual failure, promoting an increased incidence of morbidity and mortality that is resistant to current therapies.

Pathogenic events underlying PH include endothelial dysfunction, impaired nitric oxide (NO) signalling, and abnormal vessel wall proliferative responses.[5] Chronic inflammation contributes to the pathogenesis of both obesity-induced metabolic dysfunction and PH.[6] AT secretes cytokines, chemokines, and hormones, collectively referred to as adipokines, which regulate metabolic homeostasis in healthy subjects. The excess AT, in particular visceral fat, in obese individuals is linked with decreased adiponectin and increased tumour necrosis factor α (TNF-α), interleukin (IL-6), and leptin levels. This dysregulated adipokine expression, in turn, induces chronic inflammation and oxidative stress,[7] leading to pathogenic vascular and pulmonary responses. For example, elevated IL-6, TNF-α, and monocyte chemoattractant protein-1 (MCP-1) levels contribute to the pathogenesis of pulmonary arterial hypertension (PAH).[8] Plasma IL-6 levels are predictive for the severity of PH and mortality.[9] Consistent with this, mice overexpressing IL-6 in the lung display pulmonary vascular remodelling, elevated RVESP, and RV hypertrophy.[10]

Critical to both obesity-induced inflammation and PH is the enhanced generation of oxidizing inflammatory species that react with NO, limit its salutary signalling actions, promote the generation of the secondary oxidant peroxynitrite, and instigate additional pro-inflammatory signalling reactions.[11] A key source of reactive species in the intracellular and intravascular compartment is xanthine oxidoreductase (XO), which is elevated in patients with idiopathic PAH.[12] Notably, XO inhibition by allopurinol only modestly limits indices of PAH in rodent models.[13,14] Other anti-inflammatory strategies for PH, including the administration of IL-1 receptor antagonists, anti-MCP-1 gene therapy, and glucocorticoids, show only a modest therapeutic benefit. This affirms a significant unmet need for PH-targeted therapeutic agents.[8]

A common problem with most modalities for treating PH is a focus on a single molecular target that is a component of a more complex series of cascading reactions, motivating a therapeutic strategy that better addresses the multifaceted aetiology of PH. Electrophilic unsaturated fatty acids, containing oxo or nitroalkene substituents, display a broad range of adaptive signalling actions that are a consequence of an ability to modify protein structure and function. In particular, nitro-fatty acids (NO_2-FAs) are endogenously detectable products of unsaturated fatty acid reaction with NO and nitrite (NO_2^-)-derived nitrogen dioxide radical ($^{\cdot}NO_2$) that are produced during metabolic stress and inflammation.[15] The nitroalkene moiety undergoes reversible Michael addition with nucleophiles such as cysteine and histidine, promoting the post-translational modification of proteins critical to the regulation of inflammatory responses.[16] Current proteomic, genomic, and model system studies support that lipid electrophile generation links tissue metabolic and inflammatory status with adaptive gene expression.[16,17] The potential therapeutic utility of these species in limiting pathogenic responses to obesity, such as loss of insulin sensitivity and PH, is encouraged by the impact of NO_2-FAs on inhibiting vascular cell superoxide ($O_2^{\cdot-}$) and hydrogen peroxide (H_2O_2) production, limiting smooth muscle (SM) cell proliferation and improvement of endothelial function.[16–18] Mechanisms accounting for these actions include inhibition of nuclear factor kappa B (NFκB)-regulated cytokine and adhesion molecule expression, the up-regulation of anti-inflammatory transcription factor function and potent non-competitive XO inhibition.[15,16,18]

Here, we report that the administration of OA-NO_2 to a murine model of high-fat diet (HFD; 60% kcal from fat)-induced obesity improves both AT function and glucose tolerance and inhibits pro-inflammatory visceral fat and pulmonary cytokine expression, pulmonary arterial remodelling, lung macrophage infiltration, and oxidative stress. These actions, in turn, prevented increases in RVESP, PVR, and RV hypertrophy, all hallmarks of PH.

2. Methods

2.1 Animals and experimental design

All animal studies were conducted under the approval of the University of Pittsburgh Institutional Animal Care and Use Committee (protocol #1010241A). Male C57Bl/6j mice were purchased from Jackson Laboratory (Bar Harbor, ME, USA). The HFD was purchased from Research Diets Inc. (New Brunswick, NJ, USA). Obesity was induced by the HFD (D12492, with 60% of the adjusted calories derived from a fat) for 20 weeks beginning at age 6–8 weeks. Age-matched controls were maintained on a normal rodent chow (NC) diet (15% of the adjusted calories derived from fat, Pro Lab RHM 3000 rodent diet; PMI Feeds, Inc.; St Louis, MO, USA). Mice were fed *ad libitum* for 20 weeks and given free access to water. Food intake and mouse weight were monitored twice per week. At week 13.5 of the HFD study, mice were anaesthetized with isoflurane before Alzet osmotic pumps (Cupertino, CA, USA) containing vehicle (polyethylene glycol/ethanol), native oleic acid (OA), or the fatty acid nitroalkene derivative 9- and 10-nitro-octadec-9-enoic acid (OA-NO_2) were implanted subcutaneously in the back region, as previously described.[19] The osmotic mini-pump delivered a concentration of 8 mg/kg/day for OA and OA-NO_2. Febuxostat (RS026; BioTang, Waltham, MA, USA) was delivered in the drinking water (0.05 mg/mL, ~5 mg/kg/day).[20] The stability of febuxostat in the drinking water was maintained at or above 94% (capacity to inhibit XO) up to 9 days. To ensure integrity, febuxostat-containing water was replaced every 5 days. Water consumption was closely monitored to ensure no differences between treatment groups. There were three separate cohorts of mice that were randomly divided up after Week 13.5 into the following: (i) obesity/metabolic syndrome measurements (*Figures 1–3*), haemodynamic measurements (*Figures 4–5*), and haemodynamic measurements with HFD mice treated with febuxostat. For Cohort 1 (*Figures 1–3*), the number of mice were age-matched on NC ($n = 7$) and all other treatment groups on HFD were $n = 6$. For Cohort 2 (*Figures 4–5*) illustrating the pressure–volume (PV) loop haemodynamic measurements, there were age-matched on NC ($n = 6$), HFD treated with OA-NO_2 ($n = 6$), HFD alone ($n = 6$), HFD with vehicle ($n = 4$), and HFD with OA ($n = 4$). For Cohort 3 (*Figure 6*), there were two groups consisting of HFD and HFD with febuxostat ($n = 8$ for both). At Week 18.5, the glucose tolerance test (GTT) and dual-energy X-ray absorptiometry (DEXA) were performed on all cohorts with the mice being divided up so they would not get both measurements during the same week. We wanted to minimize the stress on the mice from the glucose load and the anaesthesia during the body composition

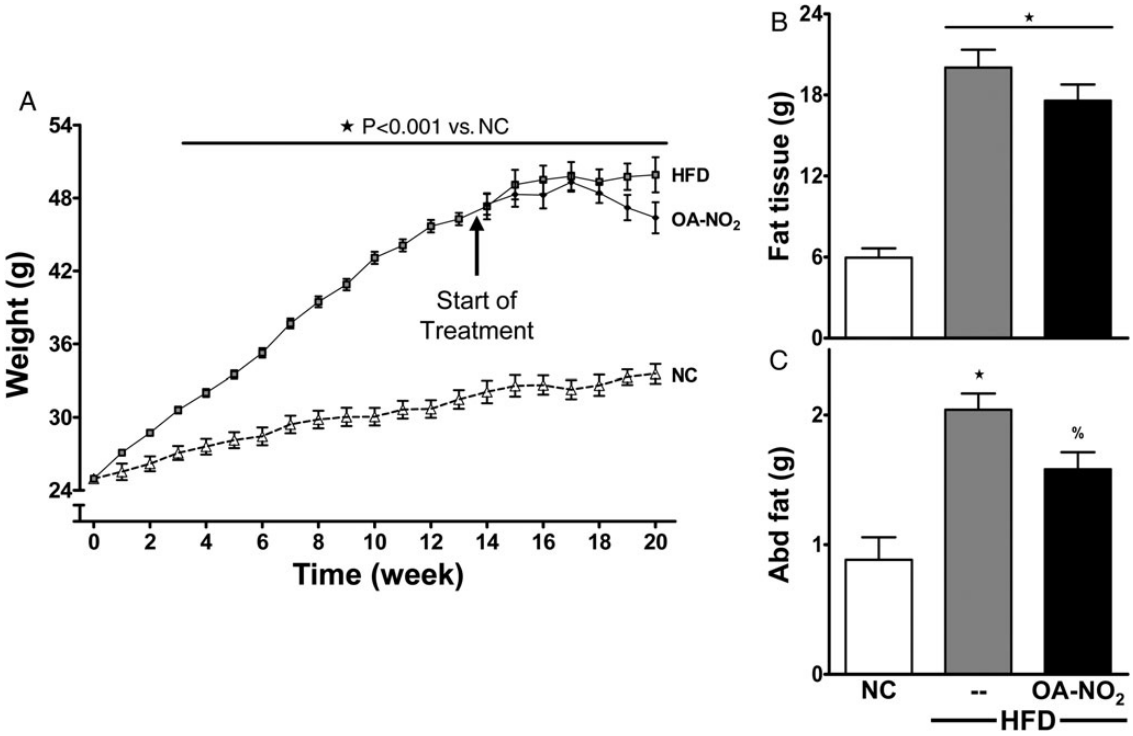

Figure 1 HFD induces weight gain and adiposity. (*A*) Mice subjected to HFD or NC were weighed weekly. (*B* and *C*) Fat tissue was determined by DEXA and abdominal fat pads were weighed at sacrifice. There was no statistical significance between HFD and HFD mice treated with OA-NO_2 for the last 6.5 weeks. Data represent mean ± SEM; ★$P < 0.001$ to NC; %$P < 0.05$ to NC; no significance between HFD and HFD + OA-NO_2 ($n \geq 6$ per group).

analysis. At the end of the 20-week study, mice were euthanized with sodium pentobarbital (100 mg/kg IP) to deeply anaesthetize and confirmed by exsanguination. For the haemodynamic studies, mice were sacrificed by a direct injection of the open chest with pentobarbital (50 μg/g) followed by iv bolus injection of 500 μL of KCl solution (pharmaceutical grade).

2.2 *In vivo* studies

Mice were fasted for 5 h for blood glucose, insulin, and GTT. Blood glucose levels were measured using a hand-held glucometer (Accu-Chek Aviva, Roche Diagnostics, Indianapolis, IN, USA). For GTT, mice were fasted and then injected intraperitoneally with filter-sterilized 1.5 g/kg glucose in 0.9% NaCl. For body composition, bone mineral density, fat mass, lean mass, and percentage of fat were determined using DEXA (GE Medical Systems, Madison, WI, USA).

2.3 Plasma collection and measurements

Mice were fasted for 5 h before all blood collections. Plasma was separated by centrifugation, aliquoted, and stored at −80°C. Insulin and leptin measurements were performed using radioimmunoassays (Vanderbilt University Hormone Assay & Analytical Services Core). Pro-inflammatory cytokines [macrophage inflammatory protein-1α (MIP-1α), IL-6, and TNF-α] and adiponectin were determined using Luminex xMAP technology (EMD Millipore, Billerica, MA, USA). The multiplex cytokine plate and singleplex adiponectin plate were measured as per the manufacturer's instructions.

2.4 Haemodynamic measurements

In vivo PV loop measurements of RV and left ventricular (LV) function were performed by an PV catheter in anaesthetized mice. Isoflurane was used throughout the procedure (5% for induction, 2% during surgery, and 1% while performing PV loop measurements). Following induction of anaesthesia, a four-electrode PV catheter (1.0 Fr, Scisense, Inc., London, ON, USA) attached to the data acquisition system (EMKA Instruments; Falls Church, VA, USA) was inserted sequentially into the apex of the RV and LV. RV and LV function were assessed under steady-state conditions and with transient inferior vena caval occlusion as previously described.[21,22] Following ventricular assessment of PV loop relationships, a 20 mHz Doppler probe was placed over the pulmonary artery and then over the aortic arch to assess CO and Doppler waveforms (DSPW; Indus Instruments, Houston, TX, USA). These assessments will be referred as PH (pre-clinical model), but the low LV pressures suggest that this is a model of PAH.

2.5 Right ventricle hypertrophy

After the heart was excised, RV hypertrophy measurement was determined by Fulton's Index. The RV wall was dissected, and the remaining LV wall and ventricular septum were weighed. Fulton's Index was calculated as the ratio of RV weight/(LV + septum weight).

2.6 Immunohistochemistry and image analysis

Lungs were perfused with phosphate-buffered saline (PBS) through the RV. Lungs were then inflated and fixed as previously described.[23] Tissues

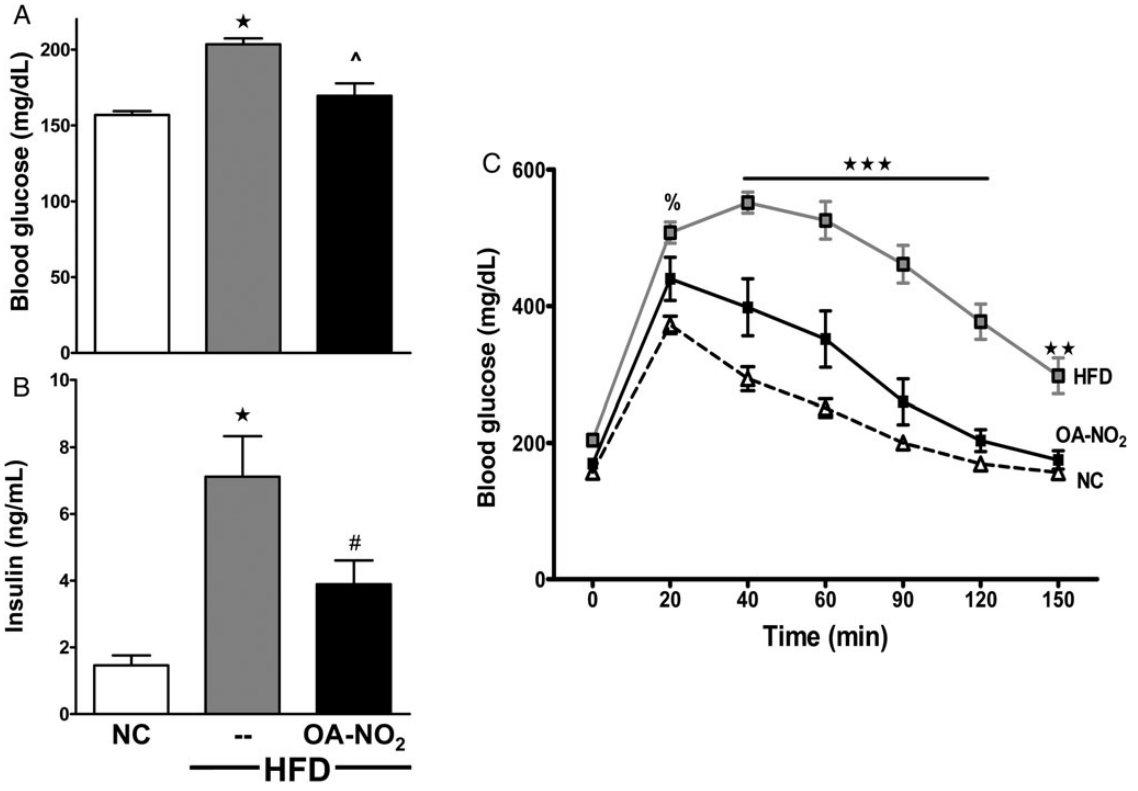

Figure 2 OA-NO_2 improves glucose tolerance. (*A* and *B*) Fasting blood glucose (*A*) and plasma insulin (*B*) levels were measured at 20 weeks. (*C*) GTT was performed with an ip injection of 1.5 g/kg glucose in 0.9% NaCl at Week 18.5. Data represent mean ± SEM; (*A* and *B*) One-way ANOVA; (*C*) two-way ANOVA; ★$P < 0.0001$ to NC; ^$P < 0.0001$ to HFD; #$P < 0.01$ to HFD; ★★★$P < 0.0001$ to NC and HFD + OA-NO_2; ★★$P < 0.01$ to NC and HFD + OA-NO_2; %$P < 0.05$ to NC; no significance between NC and HFD + OA-NO_2 at any time point ($n \geq 6$ per group).

were sectioned (7 μm), and immunohistochemical analysis was performed using anti-SM actin (SMA; C6198; Sigma, St Louis, MO, USA), anti-F4/80 (552958; BD Biosciences, San Jose, CA, USA), anti-CD31 (ab32457-100; Abcam, Cambridge, MA, USA), and/or anti-XO (200-4683; Rockland Immunochemicals, Gilbertsville, PA, USA). Confocal images were obtained using an Olympus Fluoview 1000 (Olympus, Bethlehem, PA, USA). For imaging analysis, vascular remodelling was assessed by measuring the thickness of the SM layer using the NIS Elements software (Nikon Instruments, Inc., Melville, NY, USA). Thickness measurements were made by first generating a binary mask of the SMA staining and defining the centroid region of each vessel. Lines (arm) were then drawn from this central point to the external margin of the SMA mask and the length of each arm determined by object counting. The thickness measurement for each individual vessel was comprised of an average of 15 length measurements per vessel. Two to four images (with 1–3 vessels per image) were analysed from each animal. XO abundance (anti-XO staining) and macrophage infiltration (anti-F4/80 staining) were quantified using the MetaMorph software (Molecular Devices, Sunnyvale, CA, USA) and expressed relative to nuclear counts [4′,6-diamidino-2-phenylindole (DAPI) staining].

2.7 XO activity and protein expression

Enzymatic activity was determined as previously described.[18] XO expression was assessed by Western blot using rabbit polyclonal primary (Rockland), actin (A2066; Sigma), and goat anti-rabbit secondary (32460; Pierce, Rockford, IL, USA) antibodies.

2.8 Protein carbonyl detection

The extent of protein carbonyl formation in visceral fat was assessed using the OxyBlot (Chemicon/Millipore) with modification of the manufacturer's directions. Protein carbonyls were determined by reaction of 2,4-dinitrophenylhydrazine (DNPH), yielding protein-bound 2,4-dinitrophenylhydrazones that were then detected immunologically. To avoid oxidation of proteins during handling, the manufacturer recommends adding a high concentration of thiol [either dithiothreitol (50–100 mM) or 1–2% β-mercaptoethanol (BME)] to the lysis buffer. However, the presence of adventitious metals (Fe^{3+} and Cu^{2+}), commonly encountered at up to μM levels in typical buffers, can induce further protein oxidation by rapid one-electron reduction (Fe^{3+} + reducing agent → Fe^{2+} and/or Cu^{2+} + reducing agent → Cu^{1+}) with the reducing agent (DTT or BME) and subsequent initiation of Fenton-based redox chemistry under ambient oxygen tensions. Therefore, a reducing agent was not used during the processing of samples and the samples were kept on ice to avoid artificial oxidation.

2.9 Quantitative real-time PCR

Total RNA was extracted from flash-frozen lungs using TRIzol reagent (Invitrogen, Carlsbad, CA, USA). RNA was reverse-transcribed

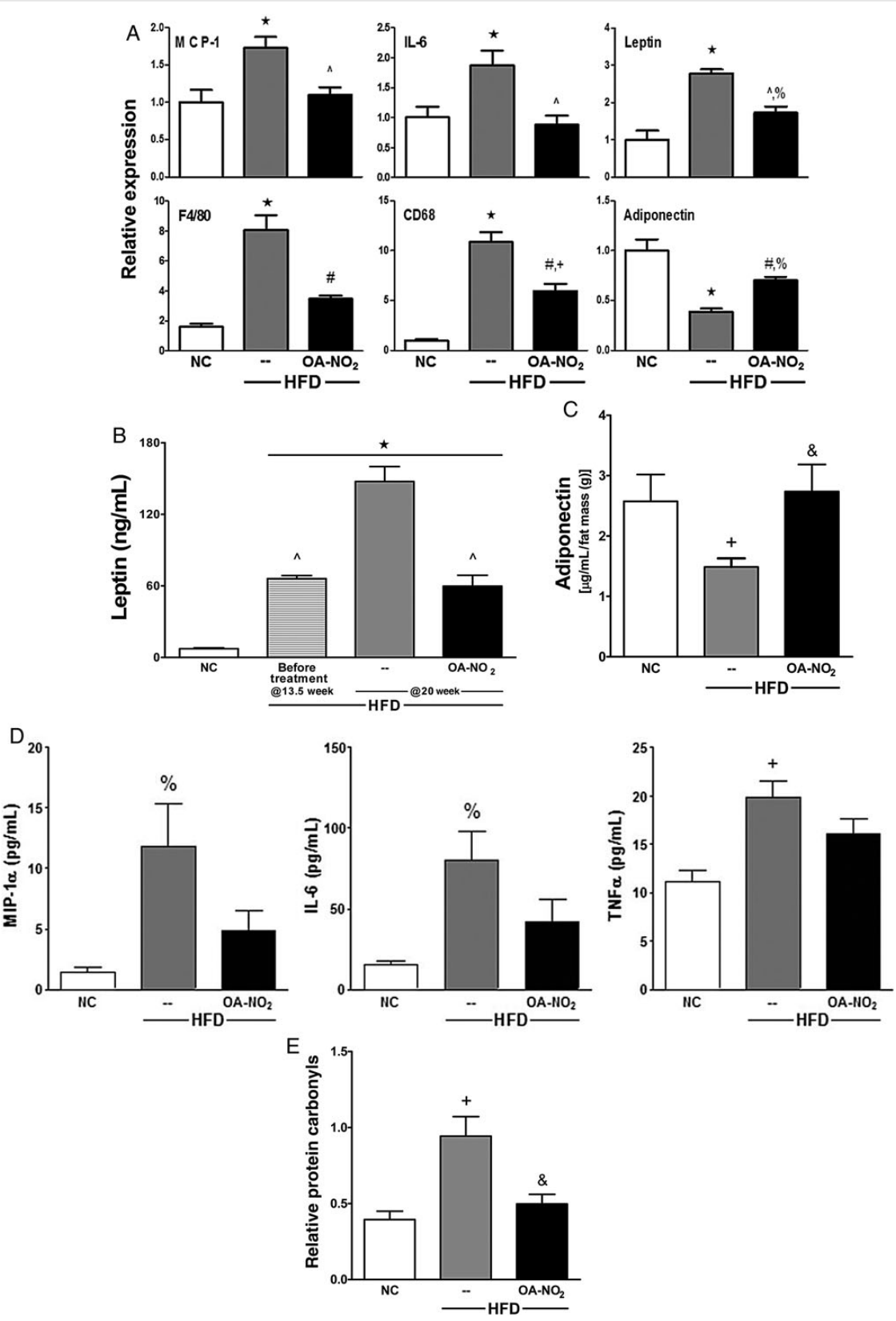

Figure 3 OA-NO_2 limits HFD-induced inflammation, normalizes adipokine levels, and prevents generation of protein carbonyls. (*A*) Pro-inflammatory cytokines (MCP-1 and IL-6), macrophage markers (F4/80 and CD68), and adipokines (adiponectin and leptin) were determined by qPCR in abdominal fat. (*B*) Circulating leptin and (*C*) adiponectin levels were measured by radioimmunoassay and Luminex singleplex, respectively. Plasma adiponectin levels were normalized to fat mass (g) determined by DEXA in Fig. 1B. (*D*) Plasma MIP-1α, IL-6, and TNF-α were measured by Luminex multiplex. (*E*) Relative protein carbonyls were determined by DNP hydrazone product detection. Data represent mean ± SEM; ★$P < 0.001$ to NC; ^$P < 0.001$ to HFD; #$P < 0.01$ to HFD; &$P < 0.05$ to HFD; +$P < 0.01$ to NC; %$P < 0.05$ to NC; no significance between NC and HFD + OA-NO_2 at any time point unless noted ($n \geq 6$ per group).

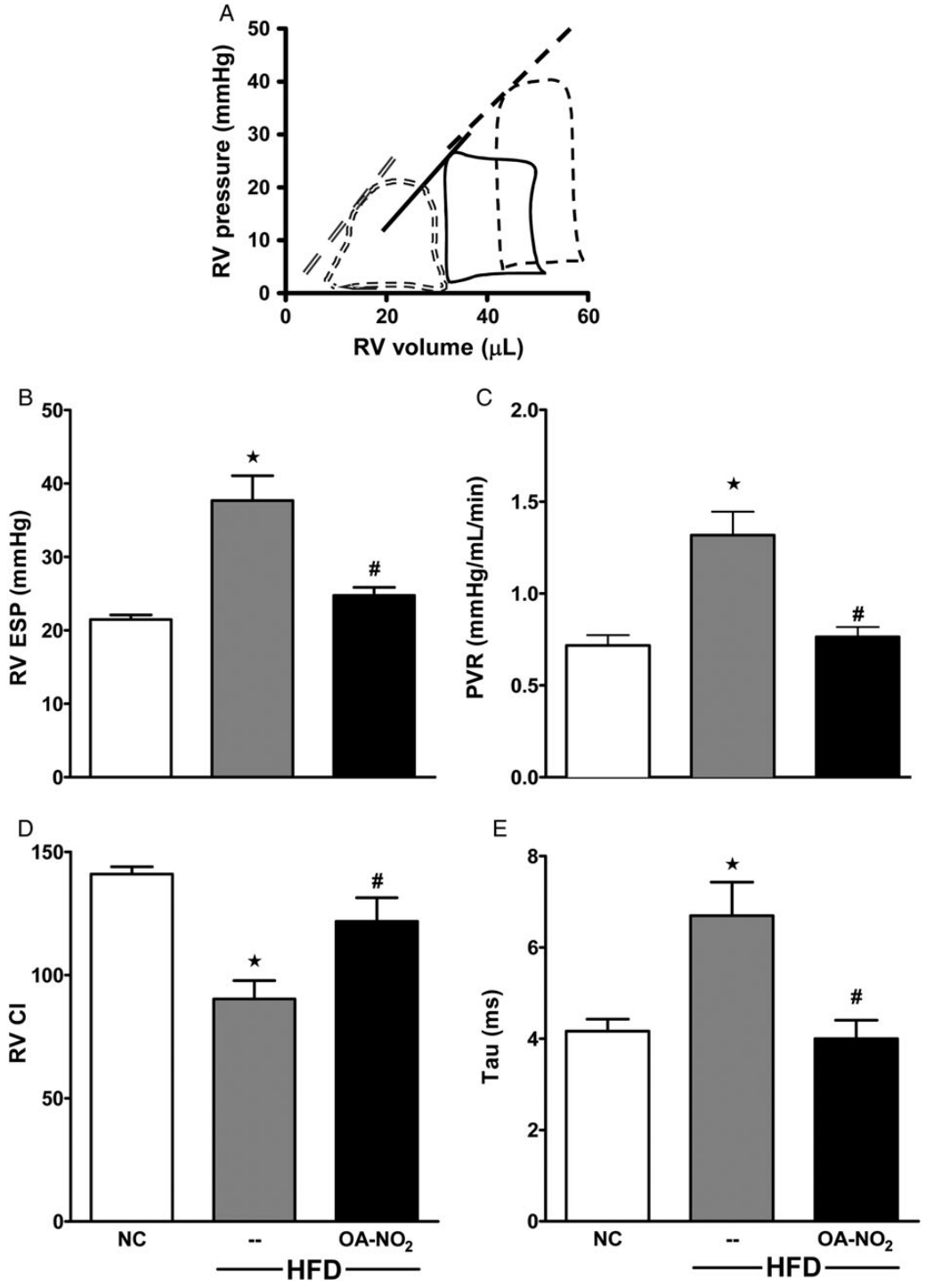

Figure 4 OA-NO_2 prevents obesity-induced PAH. (*A*) Representative tracings of PV loops in NC controls (double dashed), HFD (dashed), and HFD + OA-NO_2 groups for the last 6.5 of 20-week feeding (solid). (*B*–*E*) Haemodynamic indices were determined at 20 week in NC controls, HFD, and HFD + OA-NO_2-treated mice for RVESP (*B*), PVR (*C*), RV CI (*D*), and Tau (*E*). Data represent mean ± SEM; ★$P < 0.01$ to NC; #$P < 0.05$ to HFD; no significance between NC and HFD + OA-NO_2 ($n \geq 6$ per group).

using the iScript cDNA synthesis kit (BioRad, Hercules, CA, USA) as previously described.[19] Gene expression was determined by quantitative real-time (RT)-PCR (qPCR) using TaqMan gene expression assays-on-demand (Applied Biosystems, Foster City, CA, USA) and normalized to 18S ribosomal RNA or actin using the comparative C_t method.

2.10 Statistical analysis

Results are expressed as mean ± SEM. Statistical analysis was performed with the GraphPad Prism, and the data were analysed by one-way or two-way analysis of variance (ANOVA) with Tukey's multiple comparison *post hoc* comparisons and Student's *t*-test. All results are considered significant at $P < 0.05$.

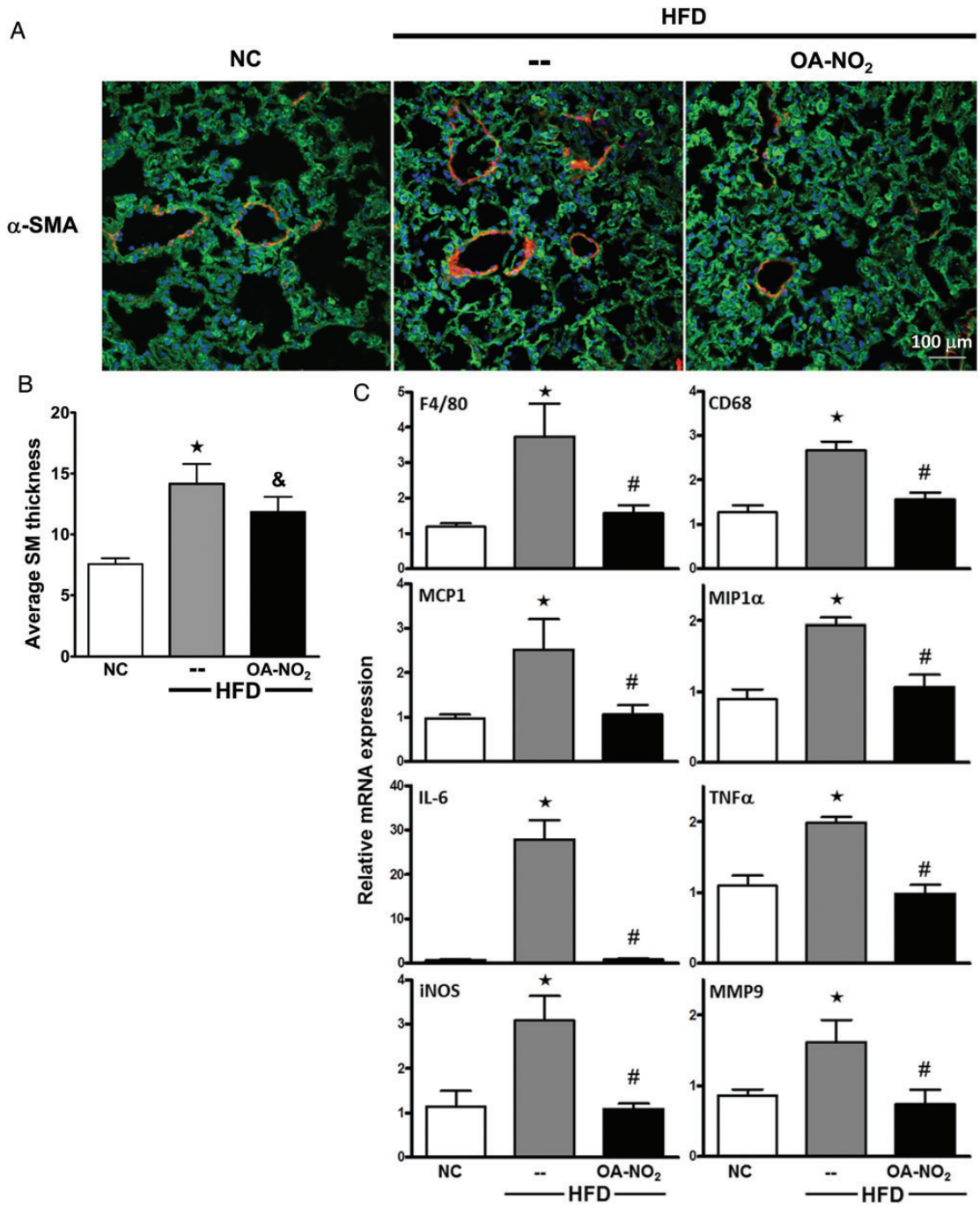

Figure 5 OA-NO_2 reduces pulmonary vascular remodelling and inflammation. (*A*) Representative confocal images of vascular remodelling stained with α-SMA and (*B*) average SM thickness of pulmonary arterioles were analysed (α-SMA, red; 4′,6-diamidino-2-phenylindole (DAPI), blue; and XO, green). (*C*) Lung inflammatory cytokine expression was determined by qPCR using Taqman assays. Data represent mean ± SEM; ★$P < 0.001$ to NC; #$P < 0.01$ to HFD; &$P < 0.05$ to HFD; no significance between NC and HFD + OA-NO_2 ($n \geq 6$ per group).

3. Results

3.1 HFD induces obesity and glucose intolerance

HFD-fed mice gained significantly more weight than the age-matched controls on NC (*Figure 1A*). The significant gain in weight was attributed to adiposity, with increased fat tissue as determined by DEXA at Week 18.5 (*Figure 1B*). Additionally, the abdominal fat pads weighed 2.3-fold more in HFD vs. NC mice (*Figure 1C*). The treatment of the electrophilic OA-NO_2 for the last 6.5 weeks did not significantly alter body weight, AT content (determined by DEXA), and abdominal fat pad weight at the end of study (*Figure 1*). In these, and all subsequent biochemical and physiological measurements, control studies showed that vehicle or native OA administration displayed no significant effect (HFD

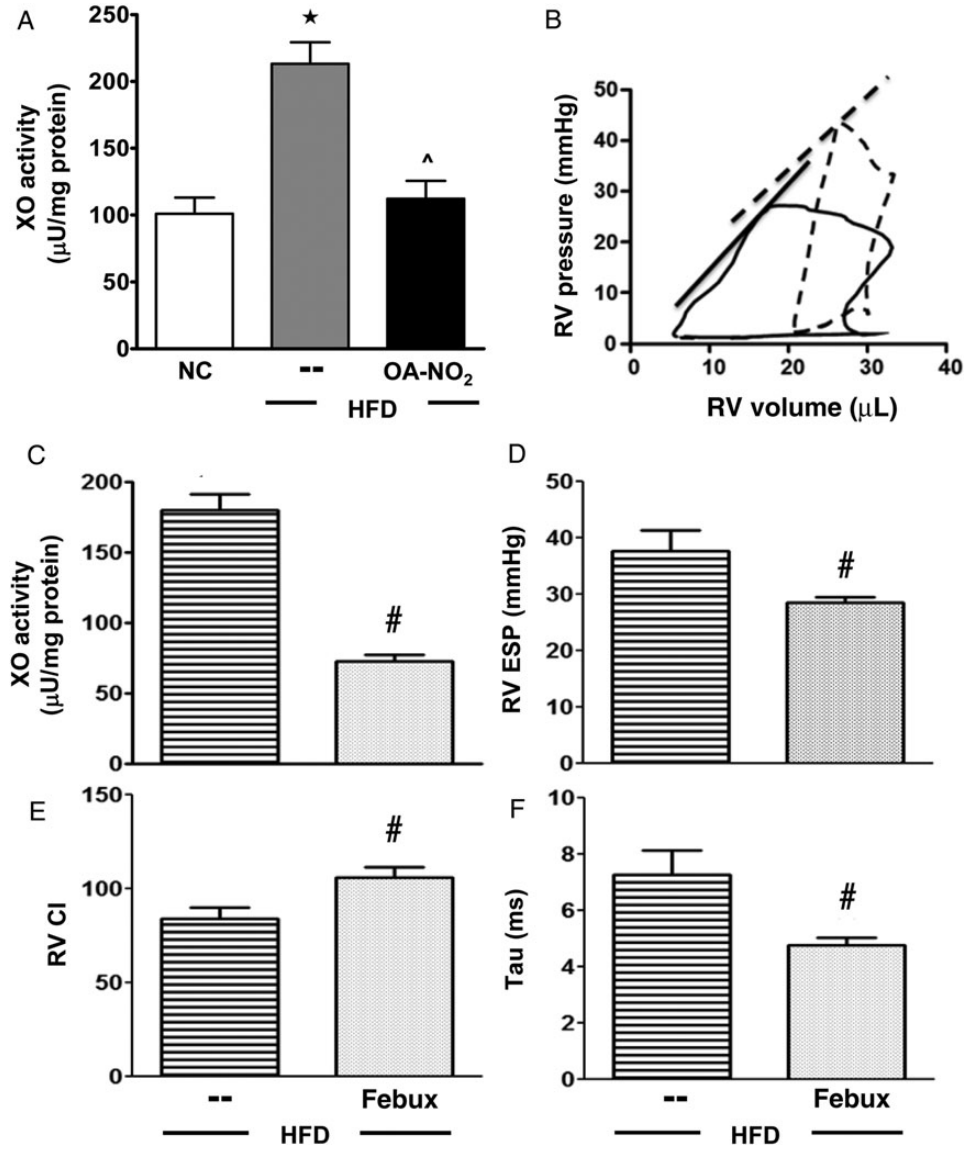

Figure 6 OA-NO_2-mediated reduction in XO activity rescues HFD-induced PAH. (*A*) Lung XO activity and (*B*) representative PV loops for HFD (dashed) and HFD + febux (solid) (*B*). (*C*–*F*) Febuxostat effects on lung XO activity (*C*), RVESP (*D*), RV CI (*E*), and Tau (*F*). Data represent mean ± SEM; (*A*) one-way ANOVA, ★$P < 0.001$ to NC; ^$P < 0.001$ to HFD; (*C*–*F*) *t*-test, #$P < 0.05$ to HFD ($n \geq 6$ per group).

without treatment, 49.9 ± 2.6; HFD with vehicle, 50.9 ± 0.9; and HFD with OA, 49.9 ± 1.0; $n \geq 6$ per group). Fasting blood glucose and insulin levels were significantly increased in the HFD mice (*Figure 2A* and *B*), and mice on HFD had impaired glucose tolerance determined by GTT (*Figure 2C*).

3.2 OA-NO_2 improves glucose tolerance

HFD-induced fasting blood glucose levels were normalized by OA-NO_2 administration, returning to levels similar to NC-fed mice (159.9 ± 2.6, NC; 203.5 ± 4.0, HFD; and 169.6 ± 2.6, HFD + OA-NO_2; *Figure 2A*). OA-NO_2 also significantly reduced blood insulin levels (1.4 ± 0.3, NC; 7.1 ± 1.2, HFD; and 3.9 ± 0.7, HFD + OA-NO_2; *Figure 2B*). The GTT revealed that HFD mice treated with OA-NO_2 disposed of the glucose load more effectively than the HFD mice, displaying a glucose tolerance that was similar to NC controls (*Figure 2C*).

3.3 OA-NO_2 limits HFD-induced inflammatory responses in visceral AT

Pro-inflammatory cytokines and adipokines synthesized and secreted from visceral ATs have been implicated in the pathogenesis of obesity-induced insulin resistance and diabetes.[1,24] Consistent with this, MCP-1 and IL-6 mRNA levels were increased in the visceral fat from HFD compared with NC, whereas OA-NO_2 treatment blocked these HFD-induced inflammatory responses. Additionally, macrophage markers (F4/80 and CD68) and leptin mRNA levels were significantly elevated in the visceral AT from the HFD mice, whereas adiponectin mRNA levels were decreased. OA-NO_2 administration increased adiponectin mRNA levels and significantly decreased macrophage infiltration and adipose leptin expression (*Figure 3A*). Consistent with this, blood leptin levels were 20-fold higher in the HFD compared with NC mice (147.5 ± 12.6 vs. 7.2 ± 0.8 ng/mL, respectively). OA-NO_2

suppressed HFD-induced leptin levels, reaching the levels observed prior to initiation of the treatment at Week 13.5 (59.7 ± 9.1 vs. 66.0 ± 2.6 ng/mL) (*Figure 3B*). Conversely, circulating adiponectin levels were significantly decreased in the HFD mice compared with NC. OA-NO_2 fully normalized the HFD-mediated decrease in plasma adiponectin levels (*Figure 3C*). In addition to HFD-induced adipokine dysregulation, systemic inflammatory cytokines were significantly increased in the plasma of HFD mice compared with NC and were also normalized by OA-NO_2 administration (*Figure 3D*). This suggests that OA-NO_2 improved AT function in HFD mice, thus normalizing pro-inflammatory cytokine, leptin, and adiponectin levels in the systemic circulation.

3.4 Oxidative stress blunted in OA-NO_2-treated HFD mice

Elevated levels and reactions of oxidative inflammatory mediators play a pathogenic role in obesity-induced metabolic syndrome. A reliable surrogate marker for oxidative stress (amino acid and lipid oxidation) is the detection of the more stable protein carbonyl derivatives via the reaction of DNPH.[25] There was an approximately two-fold increase in the oxidation of protein carbonyls from the visceral fat depot of HFD mice compared with NC, an increase that was significantly attenuated by OA-NO_2 (*Figure 3E*). This observation and the measurement of inflammatory mediators indicate that OA-NO_2 administration blunted circulating and visceral fat pro-inflammatory cytokine and adipokine levels and decreased oxidative stress in HFD mice.

3.5 HFD-induced obesity results in PH

The potential development of PH was assessed by the RV PV relationship using a micromanometer-conductance catheter inserted into the RV via the right internal jugular vein. Representative RV PV loops show a rightward shift of the end-systolic PV relationship (ESPVR) for HFD (dashed) compared with NC (double-dashed) mice (*Figure 4A*). HFD mice displayed a lower stroke volume and decreased contractility (ESPVR shifted rightward). RVESP was elevated in HFD compared with NC mice (37.7 ± 3.4 vs. 21.5 ± 1.5 mmHg, $P < 0.05$). HFD mice had increased PVR (*Figure 4C*), decreased RV systolic function [RV contractility index (CI)] (*Figure 4D*), and altered RV diastolic function (Tau, *Figure 4E*) compared with NC. Notably, there were no significant changes in LV end-diastolic pressure (LVEDP), LV CI, LV Tau, and LVESP of mice on HFD and NC (see Supplementary material online, *Table S1*). This indicates that C57Bl/6j mice consuming a HFD for 20 weeks develop physiological manifestations of PH. Additionally, this will be referred as PH (pre-clinical model), but the low LV pressures suggest that this is a model of PAH.

Table 1 Haemodynamic function in NC, HFD, and HFD treated with OA-NO_2

		HFD	
	NC	–	OA-NO_2
mPAP (mm Hg)	14.0 ± 0.3	24.6 ± 2.3★	16.6 ± 0.7#
RV Ea	0.94 ± 0.05	1.54 ± 0.19★	0.87 ± 0.12#
Fulton Index (RV/LV + S)	0.226 ± 0.008	0.272 ± 0.005★	0.226 ± 0.009#

Data represent mean ± SEM.
★$P < 0.05$ to NC; #$P < 0.05$ to HFD ($n \geq 6$ per group).

3.6 OA-NO_2 protects against HFD-induced PH

OA-NO_2 administration shifted RV PV loops back to the left in the HFD-fed mice (solid line) (*Figure 4A*). OA-NO_2 also significantly reduced RVESP (24.7 ± 1.1 mmHg) in HFD mice (*Figure 4B*, $P < 0.05$), decreased PVR to levels similar to NC-fed mice [0.76 ± 0.05 (OA-NO_2) vs. 0.72 ± 0.06 (NC), *Figure 4C*, $P < 0.05$], limited the reduction in systolic function [90.3 ± 7.4 (HFD), 121.8 ± 9.4 (HFD + OA-NO_2), and 141 ± 2.9 (NC), *Figure 4D*], and preserved diastolic function (Tau) [6.7 ± 0.7 (HFD), 4.0 ± 0.4 (HFD + OA-NO_2), and 4.2 ± 0.36 (NC), *Figure 4E*]. Changes in pressure, resistance, systolic function, and diastolic function were reflected by the HFD-induced decrease in CO, with OA-NO_2 treatment returning CO to levels reflective of NC mice (see Supplementary material online, *Table S1*). Additionally, OA-NO_2 treatment abrogated (16.6 ± 0.7) HFD-induced elevation of mean PAP [24.6 ± 2.3 (HFD) vs. 14.0 ± 0.3 (NC)]. The ratio of RVESP-to-stroke volume [effective arterial elastance (Ea), a measure of afterload[4]] was increased by HFD [1.5 ± 0.2 (HFD) vs. 0.94 ± 0.05 (NC)] and rescued by OA-NO_2 (0.87 ± 0.1). Finally, OA-NO_2 reversed HFD-mediated increases in the Fulton Index (*Table 1*).

3.7 OA-NO_2 prevents HFD-induced vascular remodelling and inflammation in the lung

Immunostaining and quantitative image analysis (*Figure 5B*, $P < 0.05$) of pulmonary arterioles for α-SMA (red) show thickened medial walls in HFD (*Figure 5A*, middle panel) compared with NC mice (left panel). This increase in SMA was significantly reduced by OA-NO_2 (right panel). Additionally, macrophage infiltration was increased in HFD lungs, a response that was significantly blunted by OA-NO_2 (F4/80 and CD68 qPCR, *Figure 5C*). The HFD also significantly induced steady-state mRNA expression of MIP-1α, IL-6, TNF-α, inducible NO synthase, and matrix metalloproteinase 9. OA-NO_2 treatment suppressed the expression of these inflammatory mediators in HFD mice to levels observed in NC-fed mice.

3.8 HFD feeding induces XO-dependent pulmonary vascular dysfunction

HFD feeding resulted in a significant increase of XO activity in the lung compared with NC (213.9 ± 6.2 vs. 101.1 ± 16.2 μU/mg protein); a response that was blocked by OA-NO_2 administration (112.3 ± 13.2 μU/mg protein), *Figure 6A*. Increases in XO catalytic activity were not paralleled by detectable increases in XO protein expression, although plasma XO levels were increased three-fold (not shown), suggesting that endothelial-bound XO may have been removed during fixation/washing. Representative RV PV loops for HFD mice (dashed) and HFD mice treated with the XO-specific inhibitor febuxostat for the last 6.5 weeks (solid) are shown in *Figure 6B*. Lung XO activity (*Figure 6C*), RVESP (*Figure 6D*), and Tau (*Figure 6F*) were significantly reduced by febuxostat compared with HFD controls. Febuxostat also improved systolic function (*Figure 6E*).

4. Discussion

The adverse impact of obesity on systemic vascular disease is well established, with the link between obesity and the development of

pulmonary vascular diseases less well defined. A pathogenic role for obesity in PH is supported by post-mortem observation of a greater prevalence of pulmonary hypertensive changes in blood vessels of obese subjects.[26] The REVEAL registry also reported a higher incidence of idiopathic PAH in overweight and obese subjects,[27] reinforcing the correlation between obesity and the development of pulmonary vascular disease. Herein, a 20-week HFD induced the development of obesity, right ventricular pathology indicative of PH, and allied inflammatory mediator expression in C57Bl/6j male mice, whereas the administration of electrophilic OA-NO_2 improved AT function and glucose tolerance, inhibited PH, and potently blocked multiple indices of inflammation.

Electrophilic unsaturated fatty acid nitroalkene derivatives are metabolic and inflammatory by-products that mediate a broad range of anti-inflammatory and vascular-protective actions due to their regulation of transcription factor and enzyme function. In particular, NO_2-FAs increase NO bioavailability via endothelial NO synthase phosphorylation, activate nuclear factor, erythroid derived 2, like 2 (Nrf2)-dependent gene expression, serve as partial agonists of peroxisome proliferator-activated receptor γ, induce heat shock factor-1 regulated gene expression, and inhibit NFκB-regulated target gene expression. The pleiotropic modulation of these signalling pathways by electrophilic lipids limits inflammation and oxidative stress, thereby promoting cardiovascular protection.[16]

Multiple sources of reactive species contribute to obesity-induced vascular pathology, including XO, NADPH oxidases, and auto-oxidation of mitochondrial respiratory chain components. In particular, XO activity is elevated in PH and its oxidant products impair NO signalling and vascular function.[12–14] The inhibition of XO using allopurinol only modestly limits PH in rodent models, possibly due to the limited capacity of allo/oxypurinol to inhibit endothelial cell-associated XO, a situation often noted during inflammatory and hypoxic conditions.[28] For example, while clinically achievable plasma allo/oxypurinol levels (~30–90 μM) successfully lower uric acid levels and alleviate gout symptoms, there is only modest inhibition of oxidant formation by XO. In addition, concentrations of allo/oxypurinol approximately four-fold greater than maximal clinical concentrations (400 μM) only modestly reduce XO activity and oxidant when XO is immobilized by endothelial cell glycosaminoglycans (GAGs). Since GAG sequestration is a key site of vascular XO compartmentalization *in vivo*, febuxostat was utilized because of more potent inhibition kinetics for both 'free' and GAG-bound XO when compared with allopurinol (~729-fold, $K_i = 0.96$ vs. 700 nM).[29] This pharmacological approach was also favoured over genetic strategies since (a) $XO^{-/-}$ and $XO^{+/-}$ mice die within 30 days after birth, and (b) inflammatory conditions promote XO release to the circulation where it can impact remote tissues, confounding the utility of tissue-specific conditional XO knockouts.[18,30]

The rationale for testing OA-NO_2 as a therapeutic for PH included: (a) superior inhibition kinetics for XO, (b) inhibition properties are not affected by the association of XO to vascular GAGs,[18] (c) a capacity to reduce inflammatory cell NADPH oxidase-dependent reactive species generation,[31] and (d) an ability to decrease pro-inflammatory gene expression[16] thereby improving vascular function and NO bioavailability. The actions of OA-NO_2 in limiting the pathobiology of obesity-induced PH are likely even more complex because of the multiple enzymatic and transcriptional regulatory mechanisms that are affected. Ongoing studies are directed towards better understanding these events in humans, in concert with dose-escalating human safety studies, using DNA and RNA sequencing strategies.

Obesity induces inflammatory responses in AT that originate from adipocytes and surrounding resident macrophages, resulting in adipose dysfunction and aberrant adipokine production.[6,7] This inflammatory milieu induces systemic inflammation through multiple signalling mediators, including increased levels of leptin, TNF-α, IL-6, vascular cell adhesion molecule, and C-reactive protein (CRP). HFD-induced adipokine dysregulation (reflected by increased circulating leptin and decreased adiponectin levels), coupled with the pro-inflammatory cytokine responses, oxidative stress, and macrophage infiltration in visceral AT (*Figure 3*) resulted in glucose intolerance (*Figure 2C*). Administration of OA-NO_2 to HFD mice blunted the expression of pro-inflammatory cytokines, macrophage infiltration, and indices of, oxidative inflammatory reactions (protein carbonyls) in visceral AT. In turn, this significantly reduced circulating pro-inflammatory cytokines and normalized circulating adipokine levels (both leptin and adiponectin), resulting in improved AT function and glucose tolerance without significantly decreasing body weight and adiposity (*Figures 1–3*). These results support that OA-NO_2 abrogates HFD-induced pro-inflammatory responses and oxidative stress, effects that may be further affected by modest but not statistically significant decreases in body weight.

By activating inflammatory mediator expression in AT, obesity also promotes insulin resistance and chronic systemic inflammation that is strongly associated with the prevalence of CVD.[1] These obesity-induced inflammatory processes mediate the initiation and progression of pulmonary vascular remodelling and increased PVR. Plasma levels of IL-6, TNF-α, and circulating CRP predict outcomes in patients with PH,[9,32] reinforcing the causal linkage between obesity, inflammation, and the development of PH.

Adipokine dysregulation has been implicated in the pathogenesis of PH.[3] For example, adiponectin knockout mice are more prone to pulmonary arterial remodelling;[33] the overexpression of adiponectin is protective in murine models of PH[34] and $apoE^{-/-}$ male mice on a HFD had significantly lower circulating adiponectin levels, insulin resistance, and developed PH.[35] Herein, HFD-mediated suppression of circulating adiponectin mRNA expression in visceral fat was blunted by the treatment of OA-NO_2. Plasma leptin levels (and mRNA levels in visceral AT) are also significantly decreased following the administration of OA-NO_2 without significant changes in adiposity (*Figure 3*). Additionally, leptin levels are elevated in idiopathic PAH patients and have been linked with endothelial dysfunction.[36] This affirms that adiponectin and leptin synthesized and secreted by the AT play an important role in the pathogenesis of PH, and the levels of these circulating adipokines are strongly modulated by OA-NO_2 administration.

Moreover, the expansion of fat mass correlates with systemic oxidative stress, both clinically and in animal models. Obesity elevates the pathogenic reactions of oxidative inflammatory mediators by increasing the rates of generation of reactive species [$O_2^{\cdot-}$, hydroxyl radical ($^{\cdot}OH$) and H_2O_2] while decreasing anti-oxidant enzyme activity (CuZnSOD and catalase).[37] Reactive species induce protein and lipid oxidation to carbonyl-containing products that can be detected by measuring the stable dinitrophenyl (DNP) hydrazone product of 2,4-DNPH reaction.[25] There was a significant increase in the oxidation of protein carbonyls (DNP hyrdrazone adduct) in visceral AT from HFD mice, when compared with NC mice (*Figure 3E*). Treating the HFD mice with OA-NO_2 significantly decreased the DNP hydrazone adducts to levels similar to those found in the age-matched NC mice.

The oxidant-generating enzymes XO and NADPH oxidase are significantly elevated in AT.[37,38] Furthermore, blocking reactive species ($O_2^{\cdot-}$ and H_2O_2) production using pharmacological inhibitors attenuate

pro-inflammatory cytokine levels, normalizes adipokine levels, and improves AT function and insulin sensitivity.[37] Additionally, XO inhibition lowered uric acid levels, decreased pro-inflammatory cytokine production in adipocytes, and reduced insulin resistance in an obese mouse model.[38] These studies coupled with our findings demonstrate that inhibiting enzymes capable of generating reactive species can greatly improve AT function and glucose tolerance.

The links between obesity and insulin resistance are well established. An accumulation of visceral AT promotes low-grade chronic inflammation, which results in insulin resistance. Elevated levels of acute phase proteins (CRP), cytokines (IL-6), chemokines (MCP-1), and adipokines (leptin) all lead to insulin resistance.[7] These pro-inflammatory responses have also been implicated in the pathogenesis of PH.[8] Moreover, insulin resistance is an important risk factor for the initiation and progression of PH, suggesting that treatments designed to improve insulin sensitivity can benefit patients with PH.[39] These findings support that insulin resistance can also contribute to the development of PH.

The connection with obesity and PH should be fairly evident; however, the links are not quite as clear clinically and in animal models possibly due to confounding issues with comorbidities. While obesity is common in the PH population,[39–41] whether obesity itself can cause PH is less well defined because glucose intolerance and/or insulin resistance are commonly linked with obesity. Thus, obesity is linked with both PH and pulmonary venous hypertension (PVH) with a majority of patients also having metabolic syndrome and/or diabetes.[42] This precept is reflected in animal models of obesity that display AT dysfunction, adipokine dysregulation, hyperglycaemia, and insulin resistance.

The current finding that OA-NO_2 has therapeutic potential in the context of obesity-induced PH is novel, although the mechanisms underlying this effect are not completely clear. In the current study, we present evidence that both adipokine dysregulation and increased oxidative stress are present in our model and can be corrected by OA-NO_2 treatment. However, our study has limitations precluding the decisive conclusion that OA-NO_2-mediated protection of adipokine function and oxidative stress are the sole pathways responsible for this effect. This study was limited in the number of experiments using the right ventricle. Further studies are planned to assess the impact of OA-NO_2 treatment on obesity-mediated alteration of redox balance in the right ventricle in order to determine whether the observed protective effects from the haemodynamic measurements (RVESP, PVR, and RV hypertrophy) could be strictly due to a decrease in oxidative stress in the right ventricle alone. Additional studies are needed to elucidate an exact signalling pathway such as the inhibition of XO using conditional XOR knockouts. These studies will determine the exact role of XO in obesity-induced PH and impaired glucose tolerance as well as the inhibitory contribution of OA-NO_2. Our previous work has demonstrated that NO_2-FAs potently activate the Nrf2 pathway.[15,16] Altering the levels of Nrf2 by either decreasing the levels using conditional knockouts of Nrf2 (or using Keap1 overexpressing mice) or by increasing the levels by overexpressing Nrf2 in particular tissues (by using Keap1 hypomorphic mice) will help shed light on the potential role of Nrf2 in our model.

In summary, mice subjected to a HFD for 20 weeks displayed an increased pro-inflammatory oxidant and pro-inflammatory cytokine/adipokine response, developed hyperglycaemia, and elevated insulin levels. Haemodynamic measurements indicated the development of PH. There were no significant changes in LVEDP at Week 20, ruling out concomitant PVH. Following the onset of obesity, OA-NO_2 administration at Week 13.5 inhibited HFD-induced pro-inflammatory cytokine/adipokine responses and improved glucose tolerance, reflected by decreased fasting blood glucose and insulin levels which coincided with protection from HFD-induced PH. These findings, coupled with the inhibition of XO-derived reactive species and oxidative stress, shed new light on a potential therapeutic strategy for PH. The pleiotropic actions of electrophilic fatty acid signalling mediators were essential in broadly limiting the adverse vascular remodelling and dysfunction in this model of obesity and PH.

Acknowledgements

We thank Janelle Stricker (West Virginia University Health Sciences Center) for technical support.

Conflict of interest: B.A.F. acknowledges financial interest in Complexa, Inc.

Funding

This work was supported by Gilead Sciences Research Scholars Program in PAH (N.K.H.K.); American Heart Association-National Scientists Development Grant—10SDG3560005 (E.E.K.); and National Institutes of Health [UO1-HL-108642-01 to H.C.C.; R01-HL-058115 and R01-HL-64937 to B.A.F.; and PO1-HL-103455 to N.K.H.K., C.M.S.C., H.C.C., B.A.F., and M.T.G.].

References

1. Berg AH, Scherer PE. Adipose tissue, inflammation, and cardiovascular disease. *Circ Res* 2005;**96**:939–949.
2. Sood A. Obesity, adipokines, and lung disease. *J Appl Physiol* 2010;**108**:744–753.
3. Summer R, Walsh K, Medoff BD. Obesity and pulmonary arterial hypertension: is adiponectin the molecular link between these conditions? *Pulm Circ* 2011;**1**:440–447.
4. Champion HC, Michelakis ED, Hassoun PM. Comprehensive invasive and noninvasive approach to the right ventricle-pulmonary circulation unit: state of the art and clinical and research implications. *Circulation* 2009;**120**:992–1007.
5. Budhiraja R, Tuder RM, Hassoun PM. Endothelial dysfunction in pulmonary hypertension. *Circulation* 2004;**109**:159–165.
6. Hotamisligil GS. Inflammation and metabolic disorders. *Nature* 2006;**444**:860–867.
7. Ouchi N, Parker JL, Lugus JJ, Walsh K. Adipokines in inflammation and metabolic disease. *Nat Rev Immunol* 2011;**11**:85–97.
8. Price LC, Wort SJ, Perros F, Dorfmüller P, Huertas A, Montani D *et al.* Inflammation in pulmonary arterial hypertension. *Chest* 2012;**141**:210–221.
9. Soon E, Holmes AM, Treacy CM, Doughty NJ, Southgate L, Machado RD *et al.* Elevated levels of inflammatory cytokines predict survival in idiopathic and familial pulmonary arterial hypertension. *Circulation* 2010;**122**:920–927.
10. Steiner MK, Syrkina OL, Kolliputi N, Mark EJ, Hales CA, Waxman AB. Interleukin-6 overexpression induces pulmonary hypertension. *Circ Res* 2009;**104**:236–244.
11. Pacher P, Beckman JS, Liaudet L. Nitric oxide and peroxynitrite in health and disease. *Physiol Rev* 2007;**87**:315–424.
12. Spiekermann S, Schenk K, Hoeper MM. Increased xanthine oxidase activity in idiopathic pulmonary arterial hypertension. *Eur Respir J* 2009;**34**:276.
13. Hoshikawa Y, Ono S, Suzuki S, Tanita T, Chida M, Song C *et al.* Generation of oxidative stress contributes to the development of pulmonary hypertension induced by hypoxia. *J Appl Physiol* 2001;**90**:1299–1306.
14. Jankov RP, Kantores C, Pan J, Belik J. Contribution of xanthine oxidase-derived superoxide to chronic hypoxic pulmonary hypertension in neonatal rats. *Am J Physiol Lung Cell Mol Physiol* 2008;**294**:L233–L245.
15. Freeman BA, Baker PR, Schopfer FJ, Woodcock SR, Napolitano A, d'Ischia M. Nitro-fatty acid formation and signaling. *J Biol Chem* 2008;**283**:15515–15519.
16. Schopfer FJ, Cipollina C, Freeman BA. Formation and signaling actions of electrophilic lipids. *Chem Rev* 2011;**111**:5997–6021.
17. Kansanen E, Jyrkkanen HK, Volger OL, Leinonen H, Kivela AM, Hakkinen SK *et al.* Nrf2-dependent and -independent responses to nitro-fatty acids in human endothelial cells: identification of heat shock response as the major pathway activated by nitro-oleic acid. *J Biol Chem* 2009;**284**:33233–33241.
18. Kelley EE, Batthyany CI, Hundley NJ, Woodcock SR, Bonacci G, Del Rio JM *et al.* Nitro-oleic acid, a novel and irreversible inhibitor of xanthine oxidoreductase. *J Biol Chem* 2008;**283**:36176–36184.
19. Khoo NKH, Rudolph V, Cole MP, Golin-Bisllo F, Schopfer FJ, Woodcock SR *et al.* Activation of vascular endothelial nitric oxide synthase and heme oxygenase-1 expression by electrophilic nitro-fatty acids. *Free Radic Biol Med* 2010;**48**:230–239.
20. Xu X, Zhao L, Hu X, Zhang P, Wessale J, Bache R *et al.* Delayed treatment effects of xanthine oxidase inhibition on systolic overload-induced left ventricular

hypertrophy and dysfunction. *Nucleosides Nucleotides Nucleic Acids* 2010;**29**:306–313.
21. Takimoto E, Champion HC, Li M, Belardi D, Ren S, Rodriguez ER *et al*. Chronic inhibition of cyclic GMP phosphodiesterase 5A prevents and reverses cardiac hypertrophy. *Nat Med* 2005;**11**:214–222.
22. Champion HC, Georgakopoulos D, Takimoto E, Isoda T, Wang Y, Kass DA. Modulation of *in vivo* cardiac function by myocyte-specific nitric oxide synthase-3. *Circ Res* 2004;**94**:657–663.
23. Khoo NKH, Cantu-Medellin N, Devlin JE, St. Croix CM, Watkins SC, Fleming AM *et al*. Obesity-induced tissue free radical generation: an in vivo immuno-spin trapping study. *Free Radic Biol Med* 2012;**52**:2312–2319.
24. Ren J. Leptin and hyperleptinemia—from friend to foe for cardiovascular function. *J Endocrinol* 2004;**181**:1–10.
25. Dalle-Donne I, Rossi R, Giustarini D, Milzani A, Colombo R. Protein carbonyl groups as biomarkers of oxidative stress. *Clin Chim Acta* 2003;**329**:23–38.
26. Haque AK, Gadre S, Taylor J, Haque SA, Freeman D, Duarte A. Pulmonary and cardiovascular complications of obesity: an autopsy study of 76 obese subjects. *Arch Pathol Lab Med* 2008;**132**:1397–1404.
27. Burger CD, Foreman AJ, Miller DP, Safford RE, McGoon MD, Badesch DB. Comparison of body habitus in patients with pulmonary arterial hypertension enrolled in the registry to evaluate early and long-term PAH disease management with normative values from the national health and nutrition examination survey. *Mayo Clin Proc* 2011;**86**:105–112.
28. Hassoun P, Yu F-S, Cote C, Zulueta J, Sawhney R, Skinner KA *et al*. Upregulation of xanthine oxidase by lipopolysaccharide, interleukin-1, and hypoxia. *Am J Respir Crit Care Med* 1998;**158**:299–305.
29. Malik UZ, Hundley NJ, Romero G, Radi R, Freeman BA, Tarpey MM *et al*. Febuxostat inhibition of endothelial-bound XO: implications for targeting vascular ROS production. *Free Radic Biol Med* 2011;**51**:179–184.
30. Ohtsubo T, Rovira II, Starost MF, Liu C, Finkel T. Xanthine oxidoreductase is an endogenous regulator of cyclooxygenase-2. *Circ Res* 2004;**95**:1118–1124.
31. Coles B, Bloodsworth A, Clark SR, Lewis MJ, Cross AR, Freeman BA *et al*. Nitrolinoleate inhibits superoxide generation, degranulation, and integrin expression by human neutrophils. *Circ Res* 2002;**91**:375–381.
32. Quarck R, Nawrot T, Meyns B, Delcroix M. C-reactive protein: a new predictor of adverse outcome in pulmonary arterial hypertension. *J Am Coll Cardiol* 2009;**53**:1211–1218.
33. Nakagawa Y, Kishida K, Kihara S, Funahashi T, Shimomura I. Adiponectin ameliorates hypoxia-induced pulmonary arterial remodeling. *Biochem Biophys Res Commun* 2009;**382**:183–188.
34. Weng M, Raher MJ, Leyton P, Combs TP, Scherer PE, Bloch KD *et al*. Adiponectin decreases pulmonary arterial remodeling in murine models of pulmonary hypertension. *Am J Respir Cell Mol Biol* 2011;**45**:340–347.
35. Hansmann G, Wagner RA, Schellong S, Perez VA, Urashima T, Wang L *et al*. Pulmonary arterial hypertension is linked to insulin resistance and reversed by peroxisome proliferator-activated receptor-gamma activation. *Circulation* 2007;**115**:1275–1284.
36. Huertas A, Tu L, Gambaryan N, Girerd B, Perros F, Montani D *et al*. Leptin and regulatory T-lymphocytes in idiopathic pulmonary arterial hypertension. *Eur Respir J* 2012;**40**:895–904.
37. Furukawa S, Fujita T, Shimabukuro M, Iwaki M, Yamada Y, Nakajima Y *et al*. Increased oxidative stress in obesity and its impact on metabolic syndrome. *J Clin Invest* 2004;**114**:1752–1761.
38. Baldwin W, McRae S, Marek G, Wymer D, Pannu V, Baylis C *et al*. Hyperuricemia as a mediator of the proinflammatory endocrine imbalance in the adipose tissue in a murine model of the metabolic syndrome. *Diabetes* 2011;**60**:1258–1269.
39. Zamanian RT, Hansmann G, Snook S, Lilienfeld D, Rappaport KM, Reaven GM *et al*. Insulin resistance in pulmonary arterial hypertension. *Eur Respir J* 2009;**33**:318–324.
40. Abenhaim L, Moride Y, Brenot F, Rich S, Benichou J, Kurz X *et al*. Appetite-suppressant drugs and the risk of primary pulmonary hypertension. International Primary Pulmonary Hypertension Study Group. *N Engl J Med* 1996;**335**:609–616.
41. Taraseviciute A, Voelkel NF. Severe pulmonary hypertension in postmenopausal obese women. *Eur J Med Res* 2006;**11**:198–202.
42. Robbins IM, Newman JH, Johnson RF, Hemnes AR, Fremont RD, Piana RN *et al*. Association of the metabolic syndrome with pulmonary venous hypertension. *Chest* 2009;**136**:31–36.